THE JOURNAL OF PHYSICAL CHEMISTRY LETTERS
A JOURNAL OF THE AMERICAN CHEMICAL SOCIETY

pubs.acs.org/JPCL

Perspective

Recent Advances and Current Challenges of High-Sensitivity Resistive Pressure Sensors for Position Recognition

Li Zhang, Rongrong Bao,* and Caofeng Pan*

Cite This: J. Phys. Chem. Lett. 2025, 16, 9169−9182

Read Online

ACCESS | Metrics & More | Article Recommendations

ABSTRACT: Innovations in sensing materials and microstructure design have led to significant progress in highly sensitive resistive pressure sensors for position recognition. Sensitive layer materials such as conductive hydrogels, carbon-based materials, MXenes, and metallic fillers have greatly enhanced sensor performance. Meanwhile, surface microstructures like domes and micropillars, along with internal porous structures, have further improved pressure sensitivity and spatial resolution. This review summarizes these recent advances and highlights future challenges such as the realization of high-density arrays, suppression of signal crosstalk, and improvements in fabrication processes.

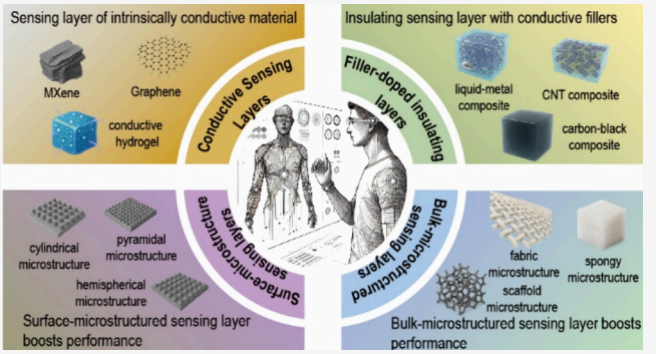

1. INTRODUCTION

In cutting-edge fields such as flexible electronics, wearable devices, and human−computer interaction, there is an urgent need for flexible pressure sensors capable of accurately sensing slight pressures and determining the location of the force.[1−5] Among various sensor types, resistive pressure sensors stand out for their simple structure, high sensitivity, and rapid response, and have thus become a hot research topic in flexible tactile sensing.[6] However, achieving both ultrahigh sensitivity and precise position resolution simultaneously remains challenging — improving an array's spatial resolution usually requires increasing the number and density of sensing units, which introduces numerous difficulties in material fabrication and array integration.[7,8] In addition, constructing large-area, high-density pressure sensor arrays presents issues such as complex fabrication processes and difficult signal readout. In terms of sensing materials, new materials such as conductive hydrogels, carbon-based conductive networks, two-dimensional MXene materials, and metal composite conductors have been developed in recent years to significantly enhance sensor performance.[9−11] At the same time, introducing microstructural designs like micropillar arrays, dome-shaped protrusions, and internal porous supports can leverage stress concentration and increased contact area to further boost the sensor's sensitivity and positional resolution.[12] Although these strategies have markedly improved the performance of flexible resistive pressure sensors, a systematic review of recent progress in this area has been lacking. This review aims to survey the latest advances in highly sensitive resistive pressure sensors for position recognition, and to analyze the key challenges currently faced along with future development directions.

2. MATERIAL-TAILORED RESISTIVE PRESSURE SENSOR ARCHITECTURES FOR POSITION RECOGNITION

2.1. Conductive Sensing Layers. In recent years, conductive hydrogels have attracted considerable attention as highly sensitive sensing layers due to their intrinsic conductivity and high flexibility. Conductive hydrogels exhibit intrinsic ionic conductivity, meaning charge can be transported by mobile ions throughout the hydrated polymer network. In addition, numerous hydrogen bonds between polymer chains and water molecules create dynamic conductive pathways that maintain electrical continuity under deformation. Owing to their soft, highly flexible matrices, these hydrogels deform easily and conform to applied pressure, which enhances contact with electrodes and promotes uniform stress distribution. Together, the ionic conduction mechanism and superior flexibility allow hydrogel-based sensors to produce large, rapid resistance changes even under slight pressures, thereby achieving high sensitivity and excellent durability over repeated loading. For example, Gao et al. developed a

Received: May 22, 2025
Revised: July 25, 2025
Accepted: July 29, 2025

https://doi.org/10.1021/acs.jpclett.5c01566
J. Phys. Chem. Lett. 2025, 16, 9169−9182

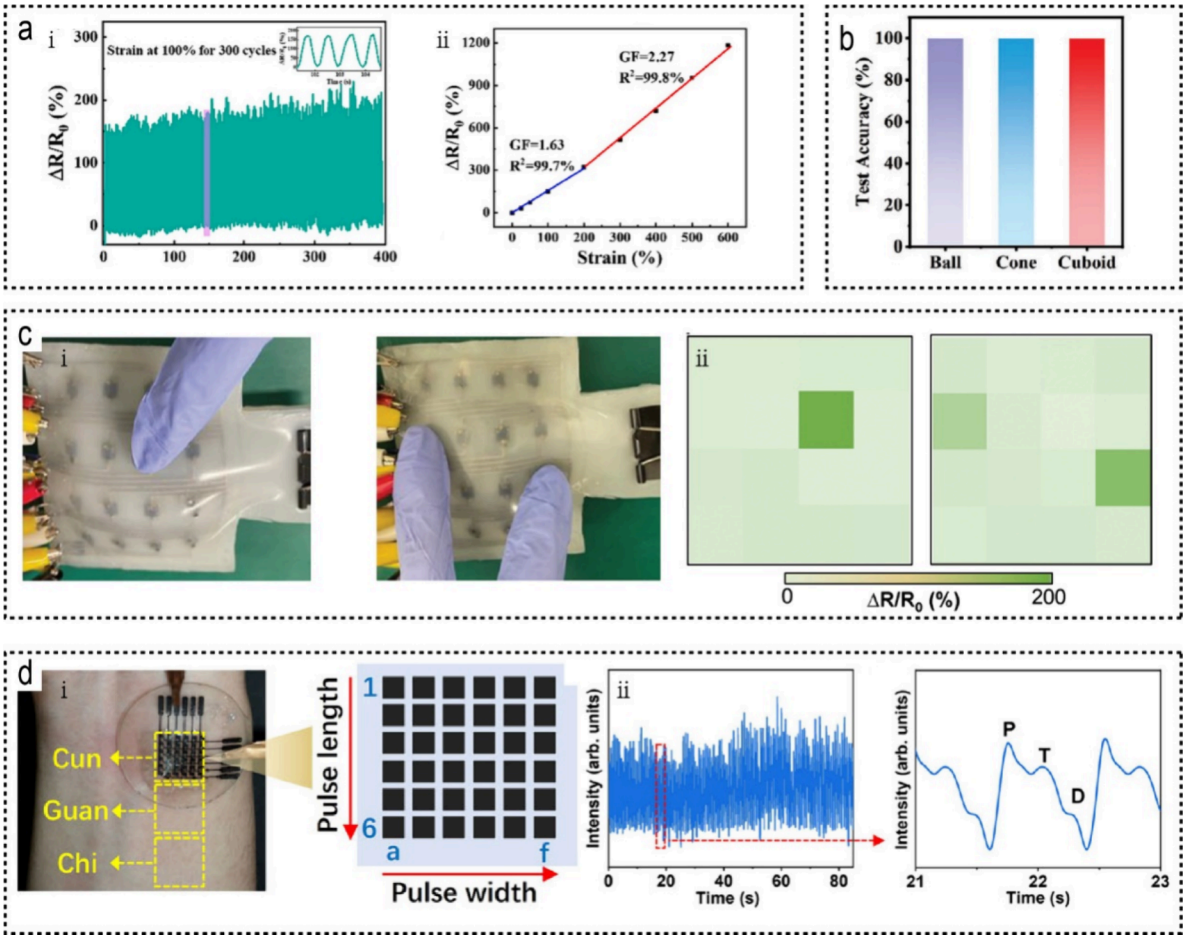

Figure 1. Representative intrinsically conductive sensing layers used in resistive pressure sensors for position recognition, highlighting durability, shape recognition, spatial pressure mapping, and pulse monitoring. (a) (i). Relative resistance changes of the PAMC-3 hydrogel under 100% strain for 300 cycles; (ii). Strain−relative resistance curve of the hydrogel.[13] (b). Accuracy of shape recognition using the trained model.[15] (c) (i). Photos of the e-skin after inflation with 80 mL of air; (ii). Pressure distribution mapping of the e-skin after inflation with 80 mL of air.[17] (d) (i). A 36-channel S-M/A1 strain sensor array was placed on the wrist above the radial artery at the Cun position to detect pulse signals; the right image shows a schematic of the sensor array with the positions of all 36 channels; sensing units are numbered 1−6 along the pulse length and a−f along the pulse width. (ii). Pulse waves continuously measured by the sensor array's 3c channel, and an enlarged view of a single pulse signal.[20]

cellulose-reinforced ionic conductive hydrogel (PAMC) that achieved a gauge factor (GF) of about 1.6 over 0−200% strain and ∼ 2.3 over 200−600% strain, with maximum stretch up to 600%. It remained operational at − 15 °C and after 300 cycles at 100% strain.[13] Similarly, Cui et al. prepared a dual-network carboxymethyl cellulose hydrogel covering an ultrawide 0−680% strain range with a GF of ∼ 2.5, a dynamic response of ∼ 0.14 s, and no notable performance degradation after 200 large-strain cycles (Figure 1a).[14] These hydrogels were antifreezing and moisture-resistant, and by using 3 × 3 sensor arrays they enabled pressure position recognition: Gao et al.'s array could discern finger taps and record the trajectory of the characters "AHU," while Cui et al.'s array rendered a three-dimensional pressure distribution spelling "DHU." Chen et al. further introduced a conductive polymer network to fabricate a glycerol-based organic hydrogel (an interpenetrating PANI−P(AAm-*co*-AAc) network) that achieved a sensitivity of 35.1 MPa^{-1} in the 0−20 kPa pressure range with a detection limit of ∼ 80 Pa, and maintained an extremely low hysteresis <3.13% even from − 18 to 60 °C and after 1000 cycles.[15] Their sensor array (a glove with a 5 × 1 strain sensing strip plus an 8-point pressure sensor on the mechanical knuckle) successfully distinguished 30°/60°/90° finger bending and, with machine learning, achieved 100% accuracy in differentiating object shapes (spherical, conical, cubic), demonstrating excellent capabilities in position and shape recognition (Figure 1b).

Carbon-based conductive networks are another important category of sensitive layers. These materials offer advantages such as widespread availability, low cost, and biocompatibility, making them an attractive choice for sensitive layers. Wu et al. used femtosecond laser ablation to pattern serpentine conductive lines with engineered cracks on carbon fiber−reinforced polymer (CFRP) films, creating an ultrasensitive strain sensor (GF up to 1227 at 0−3% strain), though with a relatively small linear range (∼7% strain).[16] This sensor responded rapidly (∼58 ms) with a strain detection limit as low as 0.04% and showed no degradation after 10,000 cycles. Wu et al. placed five such sensor elements on the knuckle joints of a glove to build a sign language translation system, achieving 98.2% and 98.9% recognition accuracy for single and continuous gestures, respectively, highlighting multipoint gesture detection and position sensing capabilities. In contrast, Li et al. developed a stretchable pressure sensor based on a 3D porous laser-induced graphene (LIG) network, with sensitivities of 2.73% kPa^{-1} below 80 kPa and 10.49% kPa^{-1} from 80−140 kPa.[17] The device had a compression response time of ∼

https://doi.org/10.1021/acs.jpclett.5c01566
J. Phys. Chem. Lett. 2025, 16, 9169−9182

70 ms, showed almost no signal drift after over 10,000 cycles, and could operate under ± 200% biaxial strain. A 4 × 4 array using the LIG sensing layer, combined with machine learning algorithms, accurately recognized different touch modes such as tapping, sliding, and grasping, and, along with flexible packaging and a Bluetooth module, enabled real-time wireless imaging of dynamic pressure distribution (Figure 1c). In addition, Tang et al. used a capillary brush coating method to prepare an ultraflat, ultrathin reduced graphene oxide (rGO) film (≈4.6 nm thick, 91.9% transparency) as a sensitive layer.[18] This sensor could detect pressures as low as 0.02 Pa and exhibited a logarithmic linear relationship between output and pressure from ∼ 0.02 Pa to 10 kPa; it had fast response/recovery times of 0.2/0.4 s under <50 Pa, and after 10,000 cycles at 35% strain its resistance drifted only 2.4%, demonstrating extremely high sensitivity, stability, and transparency.

Beyond carbon-based materials, MXene and composite conductive films have opened new avenues for sensitive layers. In particular, MXenes offer a unique combination of high electrical conductivity and mechanical flexibility, along with hydrophilic surface functional groups that enable solution processing, making them an especially appealing choice for sensitive layer applications. Yuan et al. used inkjet printing to deposit a highly conductive $Ti_3C_2T_x$ MXene film on PET, fabricating an all-resistive sensor capable of sensing both pressure and temperature.[19] The device showed a pressure sensitivity of about − 1.89% kPa^{-1} in the 0−20 kPa range (negative sign indicating resistance decreased with pressure) with a range up to 350 kPa, and response/recovery times of ∼ 50/40 ms. By exploiting MXene's negative temperature coefficient and matching it with PDMS's thermal expansion, the sensor achieved near-zero temperature drift, effectively avoiding temperature interference in the pressure signal. Yuan et al. further integrated a 3 × 3 sensor unit array (including 5 pressure and 4 temperature sensors) to image the pressure−temperature distribution when holding cold/hot objects in real time and demonstrated multimodal human−machine interaction on a smart glove. On the other hand, Liu et al. layer-by-layer assembled thiolate-terminated MXene with silver nanowires (AgNWs) to construct a flexible conductive film, where dynamic S−Ag coordination bonds under strain induced the formation of a dense nanocrack network.[20] This strain sensor covered an extremely wide 0.001%−37% strain range, with the sensitivity (GF) jumping from ∼ 500 at minute strains to over 150,000 at ∼ 35% strain. The device had an ultrafast response (∼5 ms) and excellent durability (no obvious degradation after 1000 cycles), and remained stable even at 85% relative humidity. A 10 × 10 high-density array using this sensing layer successfully achieved 3D spatiotemporal imaging of radial artery pulses and mapping of strain fields caused by tiny loads, demonstrating high-resolution position identification and potential for wearable health monitoring (Figure 1d).

2.2. Nonconductive Sensing Layers with Conductive Fillers. Nonconductive polymers or hydrogels as sensing layers can be made pressure-sensitive by introducing conductive materials to form an internal conductive network. Tang et al. blended graphene oxide (GO) with cellulose nanocrystals (CNC) and chemically reduced it to obtain a self-supporting rGO/CNC composite film, where the layered rGO built conductive pathways and the CNC served as a supporting filler.[21] Applied pressure increases layer contacts and reconstructs conductive pathways, producing a pronounced piezoresistive signal. A pressure sensor based on this film showed fast response and good stability, operating nearly linearly in the 0−10 kPa range. The authors further integrated five such sensor units on a glove to form an array, and through wireless transmission combined with a neural network algorithm, achieved high-accuracy recognition of various gestures (e.g., fist, victory sign) with over 99% accuracy. A single sensor was also used for Morse code touch input, demonstrating excellent spatial and temporal resolution. Similarly, Meng et al. adopted a double-layer bionic design: the bottom pressure-sensing layer was a graphene/PDMS conductive film on a PDMS substrate followed by a graphite-filled crack layer, and the top pressure-localization layer was a double-sided graphene/PDMS conductive film with a PDMS spacer in between, with protruding microspike-like micropillars on its surface to prevent self-adhesion and accelerate rebound.[22] This device uses crack tunneling effects in the bottom layer to produce pressure-sensitive resistance changes, and through a linear relationship between the conduction area of the top layer and the distance to the electrode, it realizes continuous pressure coordinate detection without a pixelated array, achieving a spatial resolution of ∼ 35 μm.

The combination of conductive fillers with an insulating matrix is another effective approach to impart conductivity to a sensing layer. Stevens et al. dispersed barbed nickel microparticles and eutectic gallium−indium (EGaIn) liquid metal microdroplets in PDMS, and introduced a sacrificial porogen to form an interconnected microporous structure, creating a conductive elastomer with high sensitivity over a broad pressure range.[23] The Ni particles' sharp tips achieve quantum tunneling conduction under compression, while the porous structure significantly lowers the matrix modulus; together these effects endow the sensor with keen responsiveness to tiny pressure changes. The composite showed a sensitivity of ∼ 0.313 kPa^{-1} in the low-pressure region (<50 kPa) and maintained a linear piezoresistive response even at pressures up to several MPa, with no obvious degradation after thousands of loading cycles. The authors fabricated a 3 × 3 array to demonstrate pressure distribution imaging—even when sensor units were attached to a curved surface, it accurately identified the location of applied forces, confirming its feasibility for spatial pressure mapping. In another example, Gul et al. built an internal liquid metal (Galinstan) microchannel network inside an elastomer to enable sensitive detection of pressure direction.[24] Using a 3D-printed PVA template, they performed two orthogonally arranged layers of microfluidic channels in silicone rubber and injected Galinstan, while also introducing a central domed structure to amplify deformation underload. Applied pressure reduces the cross-sectional area of the liquid metal channels, increasing resistance, and the dome converts tangential stress into normal compression, thereby enhancing sensitivity and imparting the output signal with sensitivity to the direction of pressure. By analyzing six-channel resistance signals with a convolutional neural network, the sensor could distinguish nine different load directions with over 99% classification accuracy. It was further used to remotely control a toy car's movement, demonstrating its potential in multidirectional tactile sensing applications.

Using carbon nanotubes (CNTs) as conductive fillers can likewise form effective conductive frameworks in flexible sensors. Yuan et al. dispersed multiwalled carbon nanotubes (MWCNTs) in a polyacrylamide (PAAm) hydrogel and in situ polymerized a hydrophobic elastomer coating on the hydrogel

https://doi.org/10.1021/acs.jpclett.5c01566
J. Phys. Chem. Lett. 2025, 16, 9169−9182

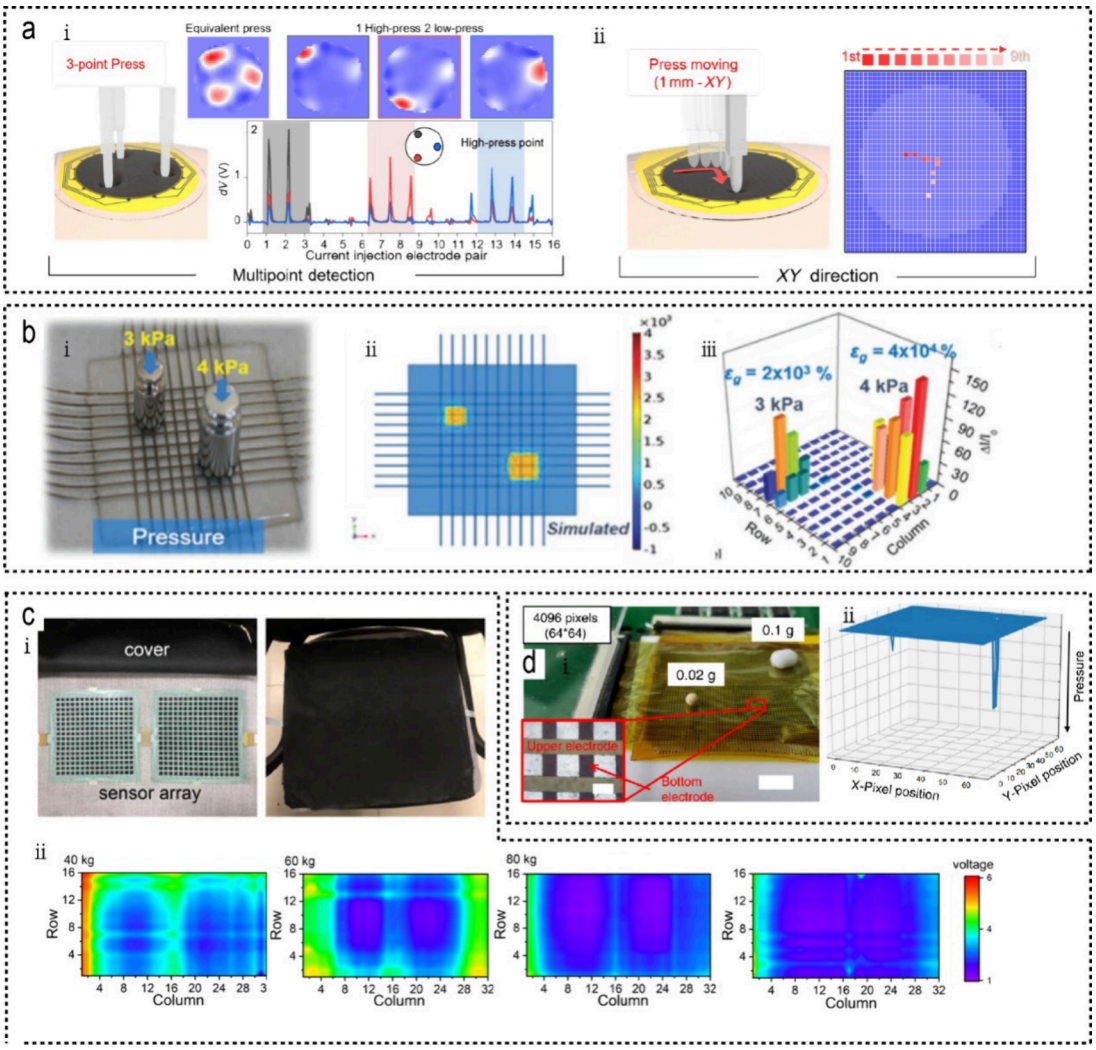

Figure 2. Representative nonconductive sensing layers with conductive fillers used in resistive pressure sensor arrays for position recognition, demonstrating multipoint mapping, load discrimination, large-area pressure distribution, and ultralight object detection. (a) (i). Multipoint tactile mapping: the e-skin simultaneously detects three separate pressure points and distinguishes their magnitudes; (ii). Spatial resolution test: a pressing load moved in 1 mm steps along the X−Y plane yields a reconstructed map with nine distinguishable pressure peak positions.[26] (b) (i). A cross-reactive sensor matrix under two localized loads (3 and 4 kPa); (ii). Simulated pressure distribution (FEA); (iii). Measured pressure distribution (with signal increases of ~ 2×10^3% and 4×10^4% for 3 and 4 kPa, respectively).[27] (c) (i). Photographs of the 16 × 32 pressure sensor array and its integration into a seat cushion; (ii). Contour plots of pressure distribution under a standard sitting posture for individuals of different body weights.[28] (d) (i). Detection of two tiny spheres (0.02 and 0.1 g) by a 64 × 64-pixel pressure sensor array, (ii). clearly distinguishing their positions and weight difference.[29]

surface, developing a flexible pressure-sensing hydrogel that resists drying and swelling.[25] The embedded MWCNTs form conductive paths within the hydrogel, while the hydrophobic encapsulation prevents water loss and volume expansion, thus maintaining stable electrical signals. This sensor remained operational under >400% tensile strain, showed ~ 7.9% resistance change at 10% strain (gauge factor ≈0.79), and exhibited no obvious drift after 1000 cycles, demonstrating excellent flexibility and durability. In comparison, Kim et al. embedded a photolithographically patterned MWCNT network between 50 μm layers of PDMS/Ecoflex and, combined with electrical impedance tomography (EIT) techniques, achieved high-resolution 3D pressure distribution imaging.[26] Local pressure increases gaps between nanotubes in the network and reduces conductive pathways, raising local impedance. Sixteen peripheral electrodes alternately injected current and measured voltage, and an EIT algorithm reconstructed a 40 × 40-pixel pressure map. For indentations up to 5 mm, the sensor's impedance increased by ~ 27.48% per millimeter (about 85% total at 3 mm), with a response time under 100 ms and no appreciable degradation after 10,000 cycles. Using a 16-electrode setup, the system could image multiple pressure points simultaneously with ~ 1 mm spatial resolution, and track moving touch points at 10 fps, enabling dynamic position sensing for handwriting trajectory recognition and even drone control (Figure 2a).

Filling an elastomer with conductive carbon black microparticles is also a common approach for constructing flexible pressure-sensing materials. Lee et al. incorporated 30 wt % conductive carbon black into a PDMS matrix as the sensitive layer, and used orthogonally arranged AgNW-coated polyurethane fibers as top and bottom electrodes, assembling a stretchable 10 × 10 piezoresistive array.[27] Mechanical strain compresses the carbon black network, reducing particle

https://doi.org/10.1021/acs.jpclett.5c01566
J. Phys. Chem. Lett. 2025, 16, 9169−9182

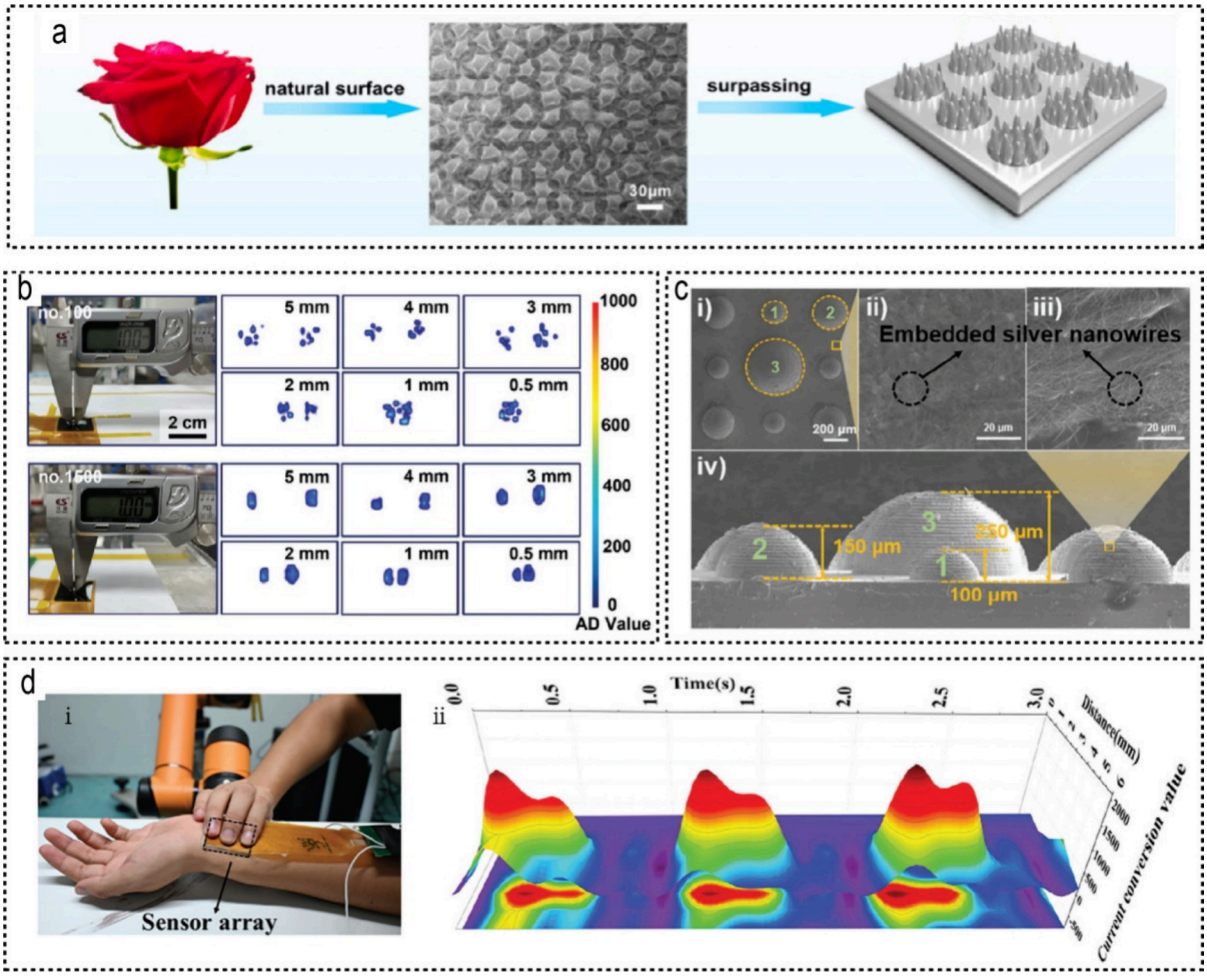

Figure 3. Representative surface microstructures used in resistive pressure sensors for position recognition, enabling enhanced sensitivity and high-resolution spatial mapping. (a) Photograph of a rose flower, the microscale dome-shaped structures on a fresh rose petal surface, and a bioinspired hierarchical array structure that surpasses the natural petal pattern.[31] (b) Spatial resolution test results of flexible pressure sensor arrays fabricated with abrasive paper #100 and #1500 microstructures. The panels show the pressure distribution when two point loads (applied via caliper tips) are separated by various distances (5 mm down to 0.5 mm); the #1500 high-consistency array clearly resolves two distinct pressure points even at 0.5 mm spacing, whereas the #100 array's pressure points merge at smaller separations.[32] (c) Dimensional illustration and SEM images of a multistage dome microstructure sensor unit. The sensing unit consists of three dome structures of different sizes (approximately 200 μm, 300 μm, and 500 μm in diameter) formed by molding, resulting in a multisize embedded dome array with good structural consistency.[35] (d) (i) Schematic of the pulse wave acquisition process using a 32 × 32 carbon-based tactile sensor array at the radial artery; (ii) spatiotemporal distribution map of the captured pulse wave, with the x-axis representing time, the y-axis representing the distance from the center of the wrist's radial artery, and the z-axis indicating pulse intensity.[41]

spacing and increasing conductive pathways, thus decreasing resistance; conversely, temperature rise causes polymer thermal expansion, increasing particle separation and raising resistance. As a result, each sensor unit can respond to both mechanical and thermal stimuli. The sensor exhibited a strain sensitivity of ~ 81.2 at 0−5% tensile strain, and a pressure sensitivity up to 264 kPa^{-1} in the low-to-medium pressure range, with response times on the order of tens of milliseconds. By scanning each node of the array and using pattern recognition algorithms, this electronic skin matrix successfully distinguished various stimuli—stretching, pressing, bending, heating, etc.—and their combinations. Each stimulus produced a distinct distribution on a 2D electrical signal heat map, demonstrating excellent position sensing and pattern recognition capabilities (Figure 2b). Additionally, Zheng et al. reported a scalable fully printed process for constructing large-area flexible pressure sensor arrays: silver paste electrodes and insulating layers were printed on a 200 μm PET substrate, a PDMS ink with 8 wt % carbon black was printed onto a waterproof fabric to replicate the woven texture as the sensitive film, and the layers were laminated to form a 16 × 32 (1024-pixel) array.[28] The fabric's woven texture imparted anisotropic microridge structures to the sensitive film, which preferentially deform under pressure to increase contact area with the electrode, significantly boosting sensitivity at low pressures. The device had a sensitivity of ~ 0.05 kPa^{-1} below 10 kPa, response/recovery times of ~ 40/100 ms, and a minimum detectable pressure of ~ 10 Pa. Using an FPGA system to read the 1024-pixel voltage map in real time, the sensing mat could discern pressure distributions of various sitting postures (standard sitting, leg-crossing, leaning) and distinguish different body weights from 40−100 kg based on output signals, demonstrating practical potential in human posture monitoring (Figure 2c).

Conductive fillers with special morphologies can even introduce entirely new sensing mechanisms. Shi et al. used spiky hollow carbon spheres (UHCS) as the conductive phase

https://doi.org/10.1021/acs.jpclett.5c01566
J. Phys. Chem. Lett. 2025, 16, 9169−9182

to fabricate a transparent, ultrasensitive pressure-sensitive film based on the Fowler−Nordheim tunneling effect.[29] The UHCS (~600 nm diameter) have sharp nanospines on their surface and, when added at <1.5 wt % into PDMS, self-assemble into an ~ 20 μm thick elastic film. Under compression, the gaps between nanospines shorten, triggering vertical tunneling conduction while the horizontal direction remains insulated. Without any micro/nanopatterning, this sensor achieved exceptionally high sensitivity and pixel density: a sensitivity of up to 260.3 kPa^{-1} at ultralow pressure of 1 Pa, remaining $\geq$ 1 kPa^{-1} in the 1−800 Pa range, and ~ 87% optical transmittance in the visible spectrum for the sensing film. Cross-electrode testing showed no signal crosstalk at 5 μm electrode spacing, enabling pressure detection at a pixel size of 25 μm^2. A 64 × 64 passive matrix array covering 32 mm × 32 mm (pixel density 400 cm^{-2}) could resolve a tiny load of 0.02 g. A statistical model projected a theoretical minimum pixel pitch of ~ 435 nm, corresponding to an extreme spatial resolution of ~ 2.7×10^6 pixels/cm^2 (≈4187 ppi) (Figure 2d).

3. MICROSTRUCTURE-ENHANCED RESISTIVE PRESSURE SENSORS FOR POSITION RECOGNITION

3.1. Surface Microstructures. Surface microstructure engineering has been widely used to improve the sensitivity of piezoresistive pressure sensors. Tan et al. bioinspired an interlocked structure of branch-like CNT electrodes and a micropillar array. Upon compression, the effective contact area increases rapidly, achieving a high sensitivity of ~ 80.8 kPa^{-1} with low hysteresis in piezoresistive response.[30] Chen et al. mimicked the dome structures on rose petals by replicating periodic semicylindrical microdomes on a PDMS substrate and coating them with MXene; in the initial state the electrode contact area is greatly reduced, but under pressure the structures deform and enlarge the contact region, thus maintaining high sensitivity over a wide pressure range (Figure 3a).[31] Such protruding microstructures (like domes or spikes) concentrate the applied stress at small points, leading to a rapid growth in true contact area even under slight pressure. Mechanically, this means a small load produces a disproportionately large change in resistance the microdome or micropillar focuses force onto a tiny region (stress concentration) and thereby amplifies the deformation and conductive contact at that spot. In essence, compared to a flat surface, a raised microdome/pillar increases the local pressure at its tip, so even a light touch yields a significant drop in resistance, greatly boosting sensitivity. For example, in biological tactile systems, microscopic surface features (such as the ridges on human fingertips) play a similar role by focusing stimuli to enhance sensory responsiveness. This bioinspired principle ensures that even gentle pressures produce pronounced electrical signals. Moreover, when such microstructures are applied to sensor arrays, they help confine each pixel's response to a small area, improving spatial resolution. By localizing the interaction and preventing pressure from spreading laterally, these surface microstructures minimize overlap of signals between neighboring pixels and reduce crosstalk in an array. For example, Zhao et al. and Yang et al. used sandpaper templates to replicate random "hedgehog" microspiked elastomer surfaces, then spray-coated them with CNT or MXene conductive layers.[32,33] When these microspikes deform under pressure, the interface contact resistance drops sharply, thereby improving low-pressure sensitivity while maintaining array uniformity (Figure 3b). Overall, the strategy of adding microstructured surfaces to the sensing layer significantly enhances the pressure responsiveness of sensors.

Beyond single-scale protrusions, multilevel or interlocked microstructure designs have also been employed to further increase sensitivity and broaden the sensing range. Zeng et al. used phase separation and femtosecond laser engraving to create ~ 15.5 μm microgroove arrays on a conductive polymer film, which, together with a graded layered conductive network, formed an interlocking interface.[34] Under pressure, conductive pathways are activated stepwise, achieving ultrahigh sensitivity on the order of 10^5 kPa^{-1} while retaining excellent linearity. Chen et al. replicated a three-level PDMS microdome array with decreasing diameters; under compression, each size of dome contacts the bottom electrode sequentially, progressively expanding the contact area (Figure 3c). This yielded a markedly increased sensitivity in the low-pressure region (~14.9 kPa^{-1}) and extended the sensing upper limit to nearly 100 kPa.[35] In such hierarchical microstructures, as pressure increases, different-sized features engage one after another. Larger structures make contact at very low pressures, and as the force rises further, smaller microfeatures begin to engage. This stepwise engagement of contact points leads to a progressive increase in conductive pathways rather than an abrupt saturation of all contacts at once. Consequently, the sensor maintains high sensitivity in the initial pressure regime and continues to respond approximately linearly over a much wider range. In other words, distributing the load across multiple structural levels alters how stress is spread through the sensor: the largest microstructures absorb the initial force and then, at higher pressures, smaller structures take on the load. This sequential deformation delays the onset of bulk stiffening and preserves a linear response across extended pressures. Another strategy is to introduce unusual force modes: Li et al. used two interlocking sliding layers of PDMS/SiO_2 microhemispheres gripping an ultrathin Au film.[36] External pressure induces tensile strain in the film rather than the conventional compressive deformation, producing a positive resistance response (i.e., the resistance increases with pressure). This overcame the sensitivity saturation bottleneck caused by material stiffening under compression, extending the sensing range into the MPa level. Additionally, Zhu et al. significantly enhanced the pressure sensitivity of a strain-based metal film sensor by etching microcavities and stress concentration holes into an elastic membrane.[37]

Many studies have further integrated microstructured sensing units into array devices to achieve high spatial resolution tactile signal acquisition and position recognition. In these designs, the incorporation of microstructures and tailored intermediate layers often serves to localize deformation within each sensing pixel. This localization prevents mechanical and electrical interference between neighboring units, enabling the array to capture fine spatial details of pressure distribution with minimal crosstalk. Bae et al. used a fiberglass mesh skeleton to pixelate the design of an 8 × 8 pressure sensor matrix with no crosstalk, successfully recognizing Braille characters.[38] Li et al. employed laser-induced graphene and serpentine support isolation to fabricate an 8 × 8 array with 0.7 mm pixel spacing, which drastically reduced row-column coupling (crosstalk < − 40 dB) and enabled tactile imaging of complex textures and localization of millimeter-scale defects.[39] Zhao et al. developed a 64 × 64 high-density array capable of clearly resolving submillimeter pressure distributions, and by using a convolutional neural

https://doi.org/10.1021/acs.jpclett.5c01566
J. Phys. Chem. Lett. 2025, 16, 9169−9182

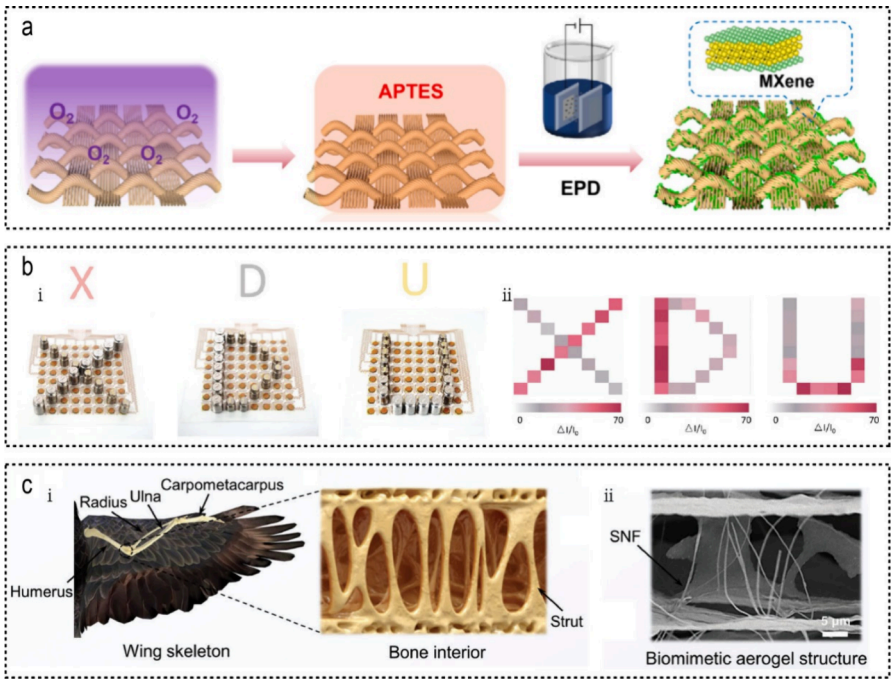

Figure 4. Representative bulk-microstructure designs in resistive pressure sensors for position recognition, featuring biomimetic architectures, array-level mapping, and lightweight aerogel scaffolds. (a) Schematic illustration of the fabrication process for a Silk/APTES/MXene sensor device;[44] (b) (i) optical images of the sensor array with 1 and 2 g weights placed to form the letters "X", "D", and "U", and (ii) the corresponding two-dimensional pressure data monitored by LabVIEW;[51] (c) (i) schematic illustrations of a bald eagle's wing skeleton and the internal structure at the end of its humerus, and (ii) an SEM image of the LSMA aerogel showing an avian bone-like microstructure.[55]

network it accurately identified complex tactile patterns (recognition rate >98%).[32] Yu et al. built a 5 × 5 hemispherical microstructure array and combined piezoresistive signals with mechano-luminescent dual-mode output to realize real-time visualization of handwriting trajectories, achieving >98% digit recognition and 97% writer identification via machine learning.[40] Tian et al.'s 32 × 32 carbon-based array achieved 3D imaging of wrist pulse waves with multipoint synchronous detection (Figure 3d).[41] Li et al. embedded a flexible microhemisphere array into an artificial knee joint prosthesis to monitor joint contact pressure distribution in real time for intraoperative mechanical evaluation.[36] Meanwhile, multifunctional integration of microstructure arrays is also advancing: Wang et al. seamlessly combined a 3 × 3 piezoresistive array with a flexible memristor array to build an "sensory-computing" electronic skin, which completed filtering and edge extraction of fingerprint-like tactile images within 0.24 ms.[42] Zhu et al. designed a 4 × 4 dual-parameter array unit that can simultaneously acquire pressure and temperature images, achieving decoupled and independent sensing of pressure−temperature signals.[37] These diverse array developments underscore that microstructure engineering at the pixel level yields high-fidelity tactile mapping and precise position recognition, even for complex multimodal sensing tasks. It highlights the critical role of microstructure design in achieving both high sensitivity and high spatial resolution for practical electronic skins.

3.2. Bulk Microstructures. Incorporating specific internal microstructures via fibrous substrates or electrospun fiber networks can significantly improve a pressure sensor's sensitivity and stability. Guo et al. coated a modal fiber fabric with a composite of 0D carbon nanoparticles and 1D carboxylated carbon nanotubes, which self-assembled (after coupling agent modification) into a hierarchical porous "hillock" microstructure.[43] Under compression, this structure greatly increases conductive contact points and shortens tunneling paths, yielding a sensitive resistive response. A flexible piezoresistive sensor based on this structure exhibited ∼ 1000.5 Pa^{-1} sensitivity in 0.1−57 kPa, a minimum detectable pressure of 0.1 kPa, and a stable working range up to 1700 kPa. The team further built a 3 × 3 unit array and used a tic-tac-toe model to verify position recognition: arrangements of pieces on different cells produced distinct resistance matrices that were completely separable via PCA clustering, and the resulting $\Delta R/R_0$ heatmaps clearly displayed the spatial pressure distribution. The array also successfully distinguished finger operations like single-click, double-click, and scroll-wheel sliding, demonstrating the feasibility of dynamic position-action recognition. Zhou et al. leveraged the naturally spiral/bundled heterogeneous fiber architecture of silk fabric: by surface-grafting 3-aminopropyl-triethoxy-silane (APTES) to uniformly fix conductive MXene nanosheets onto it, they created a flexible fabric sensitive layer with no lithography required (Figure 4a).[44] Under pressure, the spiral-bundled fibers make multiscale contact and compact together, and interlayer tunneling current is triggered between MXene sheets — both effects amplify changes in the conductive network, thereby boosting sensitivity. This fabric sensor maintained an overall high sensitivity of ∼ 17.1 kPa^{-1} over 0−3.3 MPa (reaching up to 356 kPa^{-1} in the low-pressure regime), with a detection limit of 0.25 Pa and response/recovery times of 20 ms/36 ms, and showed no signal degradation after 5000 cycles at 50 kPa. The authors combined multiple 2 cm × 2 cm sensor units into a foot plantar contour array that imaged sole pressure distributions during jumping and tiptoeing. They also placed sensor arrays on the finger,

https://doi.org/10.1021/acs.jpclett.5c01566
J. Phys. Chem. Lett. 2025, 16, 9169−9182

back of hand, face, etc., and with an MK-ResCNN deep learning algorithm achieved 95−98% recognition accuracy for sign language and lip language, showcasing the application potential of multipoint pressure sensing in human interaction.

It is worth noting that environmental factors like humidity and temperature can affect different sensor materials in distinct ways. For MXene-based sensors such as the fabric design above, a major concern is the gradual oxidation of MXene nanosheets when exposed to oxygen and moisture. High humidity or elevated temperature can accelerate this degradation of MXene, reducing its conductivity and compromising sensor performance over time. To mitigate these issues, researchers employ surface chemical treatments (for example, the APTES coupling in the silk fabric sensor helps anchor and protect the MXene layers) and encapsulation techniques to limit the material's exposure to air and water. In the case of Zhou's fabric sensor, the device showed stable operation over thousands of cycles, suggesting the MXene layer remained relatively intact during testing; however, ensuring long-term stability under prolonged high-humidity conditions would still require protective measures (such as additional sealing or antioxidation additives). By contrast, pressure sensors based on conductive hydrogels have almost the opposite dependency on the environment: they require sufficient moisture to function optimally. A hydrogel's conductivity relies on ionic movement through its hydrated polymer network, so if the surroundings are too dry or if increased temperature causes the hydrogel to lose water, the material can stiffen or its ionic conductivity can drop, leading to diminished sensor signals. Likewise, at low temperatures a hydrogel can freeze or its ions become less mobile, drastically affecting sensitivity. Researchers address these vulnerabilities by formulating hydrogels with hygroscopic or antifreeze agents (e.g., adding glycerol or salts to create an organohydrogel) and by encapsulating or packaging the hydrogel to prevent dehydration. Thus, MXene-based and hydrogel-based sensors each face distinct environmental stability challenges: MXene devices need protection from humidity and heat to avoid oxidation and conductance loss, whereas hydrogels need to retain water content and avoid extreme temperatures to remain soft and conductive. With appropriate design measures (material modifications, protective coatings, hermetic packaging, etc.), both types of sensors can be engineered for reliable operation across a range of humidity and temperature conditions.

Liu et al. used electrospinning to create a 3D polyimide (PI) nanofiber network, then deposited a thin platinum coating by magnetron sputtering to form core−shell conductive fibers.[45] The fibers' surfaces featured micro/nano dual protrusions, providing multilevel compressible conductive pathways and imparting hydrophobicity to the material. An ultrathin poly(ether imide) (PEI) film was spray-coated beneath the sensing layer as an isolation layer to reduce initial current and increase sensitivity. The sensor achieved a room-temperature sensitivity of 158.2 kPa^{-1} in 0−50 kPa, and still retained ∼ 71.5 and 113.6 kPa^{-1} at 150 °C and − 10 °C respectively, demonstrating wide-range temperature stability. It showed no performance decay after 5000 cycles (or 2500 cycles at 150 °C), and sensitivity variation was under 148 ± 10 kPa^{-1} across 30−90% relative humidity(RH). The authors fabricated a 4 × 4 array and attached the sensor units to a robotic arm gripper; even under extreme conditions—grasping at 150 °C and250 °C, holding liquid nitrogen at − 196 °C, or after 72 h of underwater immersion—the array continued to produce accurate and reliable pressure distribution readings. These results demonstrate the device's practicality for multipoint distributed pressure detection and position identification in harsh environments.

Choi et al. reported a strain-insensitive stretchable piezoresistive array: MXene suspension was coated onto reversibly cross-linked polyurethane-blend(PBU) elastic fibers (∼5 μm diameter) to form a porous conductive network, and AgNWs were spin-coated on prestretched PBU fibers to create wrinkled semicylindrical electrodes.[46] These were integrated with the sensing layer via thermal pressing to construct pressure units. Under external pressure, the contact area among conductive fibers and between fibers and electrodes increases simultaneously, causing a significant rise in current. The low-pressure sensitivity reached 888.79 kPa^{-1} (1−20 kPa) and the high-pressure sensitivity ∼ 355.56 kPa^{-1} (20−100 kPa), with a detection limit of 0.4608 Pa and response/recovery times <0.6 ms. The device showed minimal current drift after 10 loadings and 5000 stretching cycles, indicating excellent repeatability and durability. A 10 × 10 flexible array based on this design was able to map wind pressure distributions under a 3 m/s gentle breeze (capturing variations with different incident angles and distances of 20−100 mm), accurately image multipoint pressures from weights and complex models, and output virtually unchanged signals under 25% planar strain. Combined with a 1D convolutional neural network to learn array signals in 5−100 kPa, it achieved 94.1% accuracy in recognizing location and pressure levels during testing.

Moreover, Hao et al. proposed an alternately stacked TEMPO-oxidized cellulose nanofibrils (TOCNF)/MXene sensitive layer based on a Layered Arched Hierarchical Architecture (LAHA).[47] This brick-and-mortar layered microstructure, constructed by vacuum filtration to create numerous dynamic hydrogen bond bridges, not only provides continuous conductive pathways but also promotes uniform in-plane stress distribution under compression. This relieves electrode interface stress concentration and delays performance saturation. Their sensor attained a sensitivity as high as 8343 kPa^{-1} at 0−10 kPa (with optimized MXene content), a detection limit of 100 Pa, and response/recovery times of ∼ 35 ms/45 ms under a 20 kPa load, covering a working range of 0−20 kPa and showing no obvious degradation after 150,000 cycles at 15 kPa. The authors made a 6 × 6 (36-channel, 10 cm × 10 cm) tactile array with 97.2% channel response consistency, which could steadily reconstruct pressure distribution patterns of complex shapes like cones and slopes. The array's output remained nearly unchanged after 500 impacts by a 6 cm diameter, 20 g object, and it enabled multiterminal wireless synchronized monitoring both indoors and outdoors. Bending disturbances and temperature fluctuations had no significant effect on the signals. This indicates that the LAHA design effectively eliminated cross-sensitivity to common environmental and mechanical disturbances: the pressure readings remained stable despite changes in background temperature or bending strain on the device. In short, the LAHA approach produces a pressure sensor largely insensitive to ambient thermal variation, thereby focusing its response solely on applied pressure.

Introducing hierarchical cavities or support structures inside porous elastomers can similarly raise pressure sensitivity and expand linear range. Gu et al. used a two-stage foaming−

https://doi.org/10.1021/acs.jpclett.5c01566
J. Phys. Chem. Lett. 2025, 16, 9169−9182

vulcanization process to create a silicone rubber with ∼ 60% porosity and a nested "nested-cell" structure of large and small pores.[48] They then plasma-treated the pore surfaces to introduce amino groups and electrophoretically deposited acid-functionalized carbon nanotubes (FCNT), embedding them deeply inside and outside the pores to establish a conductive network in the flexible insulating matrix. Under compression, the nested-cell units undergo folding and collapse, dramatically increasing contacts between nanotubes and tunneling pathways, making resistance changes more linearly responsive. This microstructure provides >90% compressive strain capacity, overcoming the tendency of conventional high-modulus materials to saturate. The resulting sensor was only 0.76 mm thick and maintained high sensitivity over an ultrabroad 0−10 MPa range, with three linear regimes: S1 ≈ 118.9 kPa^{-1} from 0−31.25 kPa, S2 ≈ 28.3 kPa^{-1} from 31.25−500 kPa, and S3 ≈ 54.6 kPa^{-1} from 500 kPa−10 MPa, with a correlation coefficient of 0.991. The device had response/recovery times of ∼ 38 ms/42 ms, a minimum detectable pressure of 0.94 Pa, no degradation after 10,000 cycles at 5 MPa, and only 5.9% hysteresis. Xie et al. used a "salt particle template + laser ablation" method to fabricate a strain-isolated array with an island-bridge structure: first, 300 wt % NaCl particles were added to a PDMS elastomer.[49] After curing and water rinsing, a 3D porous PDMS/MWCNT conductive scaffold with 50−200 μm open pores was obtained. The entire sensing layer was then laminated with a copper electrode, and a 355 nm UV laser was used to pattern the electrode and a 1064 nm IR laser to simultaneously cut out discrete island pixels connected by elastic bridges. The internal porous microstructure causes the conductive network to rapidly reconstruct under pressure, greatly enhancing tunneling and percolation effects and raising sensitivity to 0.7702 kPa^{-1} in the 1−70 kPa range. The ultrasoft silicone (0.157 kPa) filling the pores serves as a strain buffer layer, allowing the array to operate without signal coupling even under 20% stretching. The device exhibited extremely low hysteresis up to 120 kPa, with a minimum resolvable pressure of ∼ 0.709 kPa (approximately equivalent to 1 g force) and response/recovery times of 40 ms/20 ms. The authors produced a 20 × 20 high-density array (4.8 cm × 4.8 cm) and a 32 × 32 array, successfully achieving pressure imaging of the letters "U-E-S-T-C," recognizing the sliding traces of surface textures with 3/6/9 mm spacing, and, combined with deep learning, attained 99.24% accuracy in identifying 8 types of objects gripped by a robotic hand.

Likewise, Zhu et al. used an NaCl sacrificial template to generate a highly open-cell foam in PDMS, then through poly(diallyldimethylammonium chloride) (PDDA) electrostatic self-assembly, introduced a MXene@MWCNT composite conductive network, and also embedded a 31 μm ultrathin porous PI film (0.4 mm pore diameter) between the foam and interdigitated electrodes.[50] The multilevel microstructure design gives the foam skeleton greater compressibility and stress concentration effects: the 2D MXene sheets form "fish scale" cracks upon drying, effectively modulating the opening/closing of conductive pathways. Compared to the original foam's sensitivity of 7.16 kPa^{-1}, the composite foam sensor achieved 14.16 kPa^{-1} in 0−5 kPa, expanded the linear working range to 100 kPa, and endured overloads up to 500 kPa; the detection limit was as low as 6.3×10^{-6} kPa (corresponding to 50 dB sound pressure). The device had response/recovery times of ∼ 71.4 ms/142.8 ms and showed almost no performance decay after 13,000 cycles at 5 kPa or after washing. The authors further developed a 5 × 5 pixel pressure-mapping array (10 cm × 10 cm) using porous MXene/metallic microdome (PMM) foam, integrated with an AD7606-STM32F1 wireless acquisition system. The real-time resistance matrix was transmitted via Wi-Fi to a terminal, and using custom 3D imaging software, it accurately identified the shapes and positions of various 3D-printed objects placed on the array, validating the sensor's capability for reconstructing and locating spatial pressures. Yuan et al. improved array design by adding a porous PI isolation layer and serpentine electrodes to the sensing layer, developing an array structure insensitive to bending/stretching and free of crosstalk.[51] The sensor consists of a sandwich structure: top and bottom PI/Cu electrodes, a middle sensing layer of MXene-coated nonwoven fabric, and a 30 μm thick PI insulating layer containing nine Ø0.6 mm microholes. Under pressure, the nonwoven fibers protrude to touch the electrodes and are compressed together, causing a rapid drop in resistance, while the PI isolation layer prevents direct electrode contact during minor bending and its lateral deformation along with the serpentine traces absorb ∼ 45% of tensile strain. This makes the output essentially invariant to bending curvatures <256 m^{-1} and stretching <45%. The sensor showed ∼ 21.5 kPa^{-1} sensitivity over 0.14−410 kPa, far higher than ∼ 0.16 kPa^{-1} without the isolation layer; a detection limit around 140 Pa; response/recovery of 60 ms/70 ms; pressure tolerance up to 400 kPa; no degradation over 8,000 s continuous use; and stable performance after two months. Using this design, the authors fabricated a 2 × 3 soft robotic gripper array for real-time force monitoring when grasping fruits, which showed no crosstalk even with bent fingers, and an 8 × 8 (64-pixel) array conformed on a curved display. By visualizing pixel brightness changes, it clearly displayed touch patterns like "X/D/U," with distinct brightness differences for weights of 1 g vs 2 g, indicating high spatial resolution (Figure 4b). Furthermore, quadrant mapping of the array's output signals was used to control a game character's movement, realizing position recognition under curved-surface gestures.

In summary, incorporating internal pores and structural supports within elastomer-based sensors allows a much improved balance between sensitivity and linearity. The presence of internal voids reduces the overall stiffness of the composite, making it far more compressible and enabling the sensor to sustain large deformations (often tens of percent strain) without the sharp increase in modulus that would normally cause the signal to plateau. This enhanced compressibility (particularly when pore sizes are arranged hierarchically as in the nested-cell example) permits detection of a broad pressure spectrum while maintaining high gauge factors, often manifesting as multiple linear response regions corresponding to different pore engagement stages. At the same time, spreading the applied stress across many small voids means no single region bears excessive load, which greatly improves fatigue resistance and longevity under cyclic loading. Indeed, the porous sensors described above showed negligible performance degradation over thousands of high-pressure cycles, demonstrating how internal microstructures alleviate stress concentrations and protect the material from mechanical fatigue. The characteristics of the pores(their size, shape, and distribution) are key to optimizing this effect. A combination of larger and smaller pores (i.e., a hierarchical pore structure) allows the smallest cavities to collapse and contribute to conduction at low pressures (boosting initial

https://doi.org/10.1021/acs.jpclett.5c01566
J. Phys. Chem. Lett. 2025, 16, 9169−9182

sensitivity), while the larger pores remain available to accommodate higher-pressure deformation (preserving responsiveness at elevated loads and preventing premature stiffening). Open-cell foams (interconnected pores) tend to yield low hysteresis and quick recovery because air or filler can move freely in and out of pores as they compress, whereas closed-cell pores (sealed pockets) might dampen and delay the response but can provide additional structural support at very high pressures. By tuning these parameters, designers can achieve a desired balance of sensitivity versus linear range tailored to specific application needs. In addition, integrating ultrasoft filler materials or flexible bridging structures into the porous network (as seen in some designs above) acts to buffer strain and mechanically isolate each sensing pixel. This ensures that even under substantial bending or stretching of the sensor substrate, individual sensor units maintain their integrity and do not interfere with one another. The result is that array devices with porous architectures can preserve high spatial resolution and experience virtually no crosstalk or signal drift, even under large deformations. Overall, internal microstructure engineering in elastomers (including engineered cavities, microspike infill, strain-isolation bridges, etc.) markedly enhances sensor performance and reliability, enabling high sensitivity over broad pressure ranges while ensuring that array devices remain robust and accurate under complex stress conditions.

Building sensitive layers from natural or bioinspired 3D porous scaffolds is another strategy to achieve highly sensitive, multifunctional pressure sensing. Cao et al. first delignified natural loofah sponge to retain its honeycomb tubular fiber skeleton, then fully infiltrated it with a polyacrylamide (PAM) precursor solution and introduced Fe^{3+} ions for cross-linking, obtaining an in situ polymerized PAM/Fe^{3+} composite hydrogel sensitive layer.[52] The loofah sponge's honeycomb microchannels created by delignification shorten ion migration paths and disperse stress under compression, thus improving piezoresistive sensitivity, while the 3D fiber network provides excellent mechanical support, allowing the hydrogel sensor to exhibit three linear regimes over 0−100 kPa (S1 = 2.03 kPa^{-1}, S2 = 0.51 kPa^{-1}, S3 = 0.22 kPa^{-1}) and no fatigue after 1000 cycles at 40% strain. Using this material, the authors made a 5 × 5 seat cushion array and a 16-unit insole array. The seat cushion outputs real-time pressure heatmaps for various sitting postures (sitting upright, leaning forward, leaning sideways) and, with STM32 control, provided an overlimit alert for poor posture. The insole collected plantar pressure sequences for different gaits and achieved 99.25% gait classification accuracy via machine learning, demonstrating the value of such sensor arrays in posture monitoring and position recognition. Liang et al. obtained an anisotropic layered structure "wood sponge" by chemically removing lignin and hemicellulose from balsa wood, and vacuum-infused it with reduced graphene oxide (rGO) nanosheets to build a conductive sensitive layer.[53] This layer preserved the wood's natural multilayer lamellar porous microstructure, and the rGO formed a wrinkled coating on the scaffold surfaces. Under compression, the interlayer spacing shrinks and additional conductive paths form, producing a piezoresistive response, while a temperature difference between the top and bottom surfaces generates a thermoelectric voltage signal, enabling dual pressure−temperature sensing. Because the electrical and thermal signals originate independently, they can be easily decoupled during readout. The fabricated sensor showed a bilinear response from 0.2−100 kPa (1.18 kPa^{-1} in 0−10 and 0.43 kPa^{-1} in 10−100 kPa), response/recovery of 110 ms/120 ms, a Seebeck coefficient of ∼ 27.9 μV/K, and a temperature resolution of 0.6 K. The device showed no electrical signal decay after 1000 alternating cycles of 0/10 kPa, demonstrating excellent mechanical stability and reliability. The authors set up a 4 × 4 pixel array and simultaneously recorded each pixel's resistance (pressure) and voltage (temperature) to plot 2D maps. When two 50 mL water cups (at 50 and 75 °C) were placed on different cells, the pressure distribution was identical, but the temperature distribution was clearly distinguished; when both cups were 50 °C but with 50 and 100 mL volumes, the temperature maps were similar while the pressure maps differed significantly. These results confirmed that the array can accurately distinguish pressure and temperature information at different spatial locations, meeting the requirements for multipoint tactile sensing and position recognition. The above sensors based on natural bioscaffolds, by preserving materials' unique microgeometries (e.g., honeycomb, multilayer cell walls), effectively improved the sensitivity and functional integration of flexible pressure sensing and achieved precise distributed signal acquisition in wearable human monitoring scenarios.

Using anisotropic freeze-casting−induced phase separation to construct lightweight aerogel frameworks has also provided new ideas for internal microstructured sensitive layer design. Wang et al. fabricated an oriented aerogel (PCC) composed of PEDOT:PSS/CNT/cellulose nanofibers (CNF), and built a flexible sensor with coupled piezoresistive-thermoelectric responses.[54] Water-dispersed PEDOT:PSS formed hydrogen-bonded coatings on CNFs and, together with CNTs, created a conjugated conductive network. Horizontal directional ice-templating and freeze-drying produced a layered honeycomb pore structure, followed by DMSO treatment to induce vertical phase separation of PEDOT/PSS, which improved conductivity and reduced the temperature dependence of resistance. The aerogel sensitive layer's oriented porous microstructure compresses quickly under pressure to increase conductive pathways, greatly increasing the resistance change rate; meanwhile, its extremely low thermal conductivity ensures a sizable temperature difference between layers, physically achieving complete decoupling of pressure-resistive and temperature-thermoelectric signals. The sensor's pressure sensitivity reached − 159.1% kPa^{-1} in 0−250 Pa (−24.2% kPa^{-1} in 250−1200 Pa, − 7.6% kPa^{-1} in 1200−2000 Pa), with a minimum detectable pressure of 10 Pa, response/recovery of 200 ms/150 ms, and stable performance over 1000 cycles. The temperature sensitivity (Seebeck coefficient) was up to 30.4 μV/K with 0.1 K resolution and a thermal response time of 164 ms. The authors integrated multiple PCC units into a 3 × 3 array and, with an STM32-Bluetooth circuit, achieved real-time synchronized imaging of temperature and pressure. The array successfully identified force locations and plotted temperature and pressure distributions in tests with weights and gentle finger touches/presses, and, utilizing body heat for self-powered sensing, demonstrated wireless interaction by sending "SCUT" and "0625" Morse code messages — showcasing the sensor's potential in passive human−machine interfaces. Ren et al. reported an ultralight aerogel sensor inspired by bird bone structure: by bidirectional freeze-drying, they obtained interlaced $Ti_3C_2T_x$ MXene/SiO_2 nanofiber layers, and added a small amount of PVA as molecular glue to strengthen interlayer bonding, constructing a MXene conductive aerogel with a bioinspired "lamella-beam" support

https://doi.org/10.1021/acs.jpclett.5c01566
J. Phys. Chem. Lett. 2025, 16, 9169−9182

(Figure 4c).[55] This bird-bone-like internal microstructure allows each layer and pillar to share stress under compression, avoiding local collapse and instability, greatly improving the aerogel's compressibility and fatigue life (after 10,000 cycles at 50% compressive strain, height retention was 99.1%). Thanks to MXene's high conductivity, the sensitive layer forms more conductive pathways upon compression, producing a piezoresistive effect; simultaneously, temperature differences between layers trigger a thermoelectric voltage in MXene. The two signals do not couple, enabling decoupled dual-modal pressure and temperature sensing. The device showed a piezoresistive sensitivity of about $-0.94\ kPa^{-1}$ in 0.20−0.67 kPa (negative sign indicating resistance drop with pressure) with a minimum detectable pressure of 0.20 Pa, and response/recovery times of 66 ms/36 ms, covering a range of 0−5 kPa. The temperature channel had a Seebeck coefficient of $-8.96\ \mu V/K$ and a temperature difference resolution of 0.07 K, with a response time of 0.68 s, and showed essentially no change in thermoelectric output under 0−1000 Pa pressure or in piezoresistive output under 0−40 K temperature differences, confirming complete independence of the two signals. A 5 × 5 electronic skin array based on this aerogel could simultaneously image planar pressure and temperature distributions, and a smaller 3 × 3 array, combined with a convolutional neural network, realized a dual multidigit tactile encrypted input ("1579/2468" entered via simultaneous multipoint touches) with 100% recognition accuracy, demonstrating secure communication in human−machine interaction. Array tests covered scenarios ranging from a sliding finger touch, to detecting the approach of hot or cold objects, and even sensing suspended objects without direct contact, showcasing the great potential of this sensor design for spatial position recognition and for secure, multimodal sensing.

Therefore, by employing advanced internal architectures (whether the layered, arched polymer/MXene network of a design like LAHA, or the ultralight bioinspired aerogel frameworks described above) sensors can maintain high sensitivity and even gain new functionalities while effectively minimizing cross-sensitivity between different stimuli. The LAHA approach, for instance, yields a pressure sensor that is intrinsically stable against temperature changes (virtually no thermal drift in its output), whereas the thermoelectric aerogel strategies provide entirely separate output channels for pressure and temperature, thereby completely eliminating interference between the two measurements. The array implementations of these strategies have successfully demonstrated precise capture and identification of multidimensional information, which is of great significance for the development of future intelligent electronic skins and secure human−machine interactions.

Finally, beyond the material and structural approaches discussed, additive manufacturing (3D printing) techniques are emerging as a powerful tool to directly create microstructured pressure sensors with enhanced design flexibility and scalability. Through 3D printing, complex microarchitectures can be fabricated on or within the sensor substrate (for example, arrays of micropillars or domed protrusions, internal lattice networks, or custom porous infill patterns) without the need for traditional lithographic molds. The printing process itself (whether extrusion-based, inkjet deposition, or a light-based method like stereolithography) influences the geometry and surface finish of the resulting microstructures, which in turn affects sensor performance. For instance, the layer-by-layer deposition inherent in 3D printing can be tuned to introduce fine internal channels or controlled pore structures that modify the sensor's compressibility and sensitivity. Slight variations in print resolution or curing parameters will alter the shape and roughness of each printed microfeature, thereby adjusting how those features come into contact and form conductive pathways under pressure. One key advantage of 3D printing is the ability to rapidly prototype and customize the sensor layout: engineers can easily adjust microstructural dimensions in a digital model (such as pillar height/spacing, lattice density, or pore size) to target a desired sensitivity or pressure range, then fabricate that design on demand. This greatly accelerates design iteration and optimization compared to time-consuming conventional fabrication. Furthermore, 3D printing offers a clear route to scalability − multiple sensor units or a large-area array can be printed in a single batch, enabling high-throughput manufacturing of dense sensor networks. It is also feasible to print on curved or flexible substrates, integrating sensors directly into nonplanar surfaces for applications on robotic limbs, body-worn devices, or irregular structures. Additionally, 3D printing's multimaterial capabilities allow conductive inks and insulating or support materials to be printed together in one process, so structural elements, electrodes, and even encapsulation features can be created in a single manufacturing step. Overall, the adoption of 3D printing in sensor fabrication can streamline the creation of tailored microstructures and open up new possibilities for complex designs, paving the way for scalable production of high-performance pressure sensors with application-specific geometries and functionalities.

4. CONCLUSION AND FUTURE PERSPECTIVES

Significant strides have been made in high-sensitivity resistive pressure sensors for position recognition through both advanced materials and innovative microstructures. However, achieving an ideal sensor that is durable, eco-friendly, biocompatible, highly sensitive, stretchable, high-resolution, flexible, and versatile requires a synergistic integration of material selection and microstructure design. No single

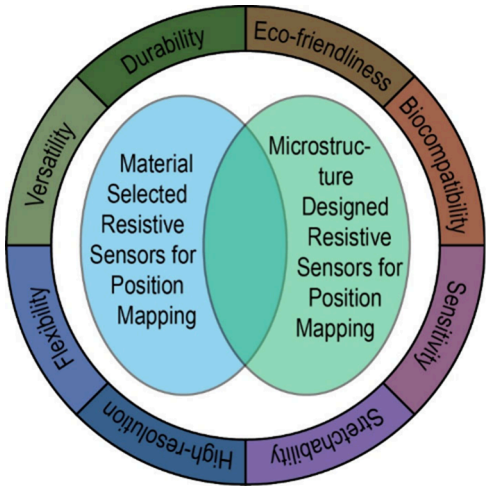

Figure 5. Current conflicts and future prospects of resistive pressure sensors for position recognition. Balancing durability, eco-friendliness, biocompatibility, sensitivity, stretchability, high resolution, flexibility, and versatility hinges on integrated material-selection and microstructure-design strategies that reconcile these inherent trade-offs.

https://doi.org/10.1021/acs.jpclett.5c01566
J. Phys. Chem. Lett. 2025, 16, 9169−9182

approach can optimize all properties simultaneously, and some performance goals are inherently at odds: for example, maximizing sensitivity often compromises spatial resolution, and achieving extreme stretchability can undermine long-term durability. Balancing these trade-offs demands integrated design strategies that carefully harmonize material and structural innovations (Figure 5).

Looking forward, future research should focus on material innovation (developing new conductive composites, more stable, sustainable and biocompatible materials, and self-healing systems) and microstructure engineering (creating hierarchical, multiscale architectures to boost sensitivity without sacrificing resolution or robustness). Equally important is system integration, including improved array design and readout architectures to minimize crosstalk, and application-driven design optimization. By tailoring sensor systems to the needs of wearables, medical monitoring, and human−machine interaction, researchers can ensure that these high-performance pressure sensors achieve widespread adoption — enabling smarter wearable electronics, advanced healthcare monitoring, and more intuitive human−machine interfaces.

AUTHOR INFORMATION

Corresponding Authors

Caofeng Pan − *School of Chemistry and Chemical Engineering, Guangxi University, Nanning, Guangxi 530004, P. R. China; Institute of Atomic Manufacturing, Beihang University, Beijing 100191, China; International Research Institute for Multidisciplinary Science, Beihang University, Beijing 100191, China;* orcid.org/0000-0001-6327-9692; Email: pancaofeng@buaa.edu.cn

Rongrong Bao − *Institute of Atomic Manufacturing, Beihang University, Beijing 100191, China; International Research Institute for Multidisciplinary Science, Beihang University, Beijing 100191, China;* orcid.org/0000-0003-1145-6882; Email: baorongrong@buaa.edu.cn

Author

Li Zhang − *School of Chemistry and Chemical Engineering, Guangxi University, Nanning, Guangxi 530004, P. R. China;* orcid.org/0009-0007-5061-8262

Complete contact information is available at: https://pubs.acs.org/10.1021/acs.jpclett.5c01566

Notes

The authors declare no competing financial interest.

Biographies

Professor Caofeng Pan is a distinguished Professor at Beihang University, and awardee of the National Science Fund for Distinguished Young Scholars. Prof. Pan earned his bachelor's (2005) and doctoral (2010) degrees from Tsinghua University. He subsequently worked at the Georgia Institute of Technology and Chinese Academy of Sciences from 2010 to 2023. Currently, he is a full professor at the Institute of Atomic Manufacturing, Beihang University. Prof. Pan's research focuses on atomic-level manufacturing and low-dimensional semiconductor materials/device. He has authored over 355 peer-reviewed publications with an h-index of 100, and been identified as a Highly Cited Researcher by Clarivate (2023-2024). Group website: https://www.piezotronics.cn.

Rongrong Bao is a Professor at Beihang University. She primarily engages in research on organic/inorganic hybrid optoelectronic devices, flexible sensors, and bionic intelligent tactile systems. She has published over 40 SCI papers in Nature Communications, Science Bulletin, Advanced Materials, etc., amassing >3,800 citations. One paper was selected as an ESI Highly Cited Paper and among "China's 100 Most Influential International Academic Papers" (2018). She has filed 14 Chinese patents, 7 of which have been granted. Her honors include the 2019 MINE Young Scientist Award and the First Prize of the Henan Provincial Natural Science Award (Rank 7/9).

Li Zhang is a Ph.D. candidate at the College of Chemistry and Chemical Engineering, Guangxi University, and has been jointly trained at the Beijing Institute of Nanoenergy and Nanosystems since 2016. He earned his Bachelor's degree from the School of Optoelectronic Information at Chongqing University of Technology in 2010, and pursued his Master's degree at the College of Electronic Engineering and Technology, Chongqing Normal University from 2015 to 2018. His research focuses on integrating flexible displays with high-resolution pressure sensors.

ACKNOWLEDGMENTS

The authors thank the support of Natural Science Foundation of China (52192610, 62422120, and 52371202) and Natural Science Foundation of Beijing Municipality (L223006).

REFERENCES

(1) Dai, Z.; Wang, M.; Wang, Y.; Yu, Z.; Li, Y.; Qin, W.; Qian, K. A smart finger patch with coupled magnetoelastic and resistive bending sensors. *Journal of Semiconductors* **2025**, *46* (1), 012601.

(2) Hu, Y.; Zhang, Q.; Han, J.; Lian, X.; Lv, H.; Pei, Y.; Shen, S.; Liang, Y.; Hu, H.; Chen, M.; Mo, X.; Chu, J. Recent progress on stability and applications of flexible perovskite photodetectors. *Journal of Semiconductors* **2025**, *46* (1), 011601.

(3) Xia, K.; Wu, W.; Zhu, M.; Shen, X.; Yin, Z.; Wang, H.; Li, S.; Zhang, M.; Wang, H.; Lu, H.; Pan, A.; Pan, C.; Zhang, Y. CVD growth of perovskite/graphene films for high-performance flexible image sensor. *Sci. Bull. (Beijing)* **2020**, *65* (5), 343−349.

(4) Liu, J.; Zhang, Z.; Qiao, S.; Fu, G.; Wang, S.; Pan, C. Lateral bipolar photoresistance effect in the CIGS heterojunction and its application in position sensitive detector and memory device. *Sci. Bull. (Beijing)* **2020**, *65* (6), 477−485.

(5) Ge, G.; Lu, Y.; Qu, X.; Zhao, W.; Ren, Y.; Wang, W.; Wang, Q.; Huang, W.; Dong, X. Muscle-Inspired Self-Healing Hydrogels for Strain and Temperature Sensor. *ACS Nano* **2020**, *14* (1), 218−228.

(6) Huang, J.; Guo, Y.; Jiang, Y.; Wang, F.; Pan, L.; Shi, Y. Recent advances and future prospects in tactile sensors for normal and shear force detection, decoupling, and applications. *Journal of Semiconductors* **2024**, *45* (12), 121601.

(7) Lu, Y.; Qu, X.; Zhao, W.; Ren, Y.; Si, W.; Wang, W.; Wang, Q.; Huang, W.; Dong, X. *Highly Stretchable, Elastic, and Sensitive MXene-Based Hydrogel for Flexible Strain and Pressure Sensors*; Research (Wash DC) 2020; Vol. *2020*, p 2038560.

(8) Liu, Y.; Bao, R.; Tao, J.; Li, J.; Dong, M.; Pan, C. Recent progress in tactile sensors and their applications in intelligent systems. *Sci. Bull. (Beijing)* **2020**, *65* (1), 70−88.

(9) Yin, R.; Li, L.; Wang, L.; Lou, Z. Self-healing Au/PVDF-HFP composite ionic gel for flexible underwater pressure sensor. *Journal of Semiconductors* **2023**, *44* (3), 032602.

(10) Zhao, Y.; Gao, W.; Dai, K.; Wang, S.; Yuan, Z.; Li, J.; Zhai, W.; Zheng, G.; Pan, C.; Liu, C.; Shen, C. Bioinspired Multifunctional Photonic-Electronic Smart Skin for Ultrasensitive Health Monitoring, for Visual and Self-Powered Sensing. *Adv. Mater.* **2021**, *33* (45), No. e2102332.

(11) Zhang, Q.; Zuo, S.; Chen, P.; Pan, C. Piezotronics in two-dimensional materials. *Infomat* **2021**, *3* (9), 987−1007.

(12) Shi, Y.; Zhang, Z.; Huang, Q.; Lin, Y.; Zheng, Z. Wearable sweat biosensors on textiles for health monitoring. *Journal of Semiconductors* **2023**, *44* (2), 021601.

(13) Gao, J.; Li, X.; Xu, L.; Yan, M.; Bi, H.; Wang, Q. Transparent multifunctional cellulose-based conductive hydrogel for wearable strain sensors and arrays. *Carbohydr. Polym.* **2024**, *329*, 121784.
(14) Cui, L.; Wang, W.; Zheng, J.; Hu, C.; Zhu, Z.; Liu, B. Wide-humidity, anti-freezing and stretchable multifunctional conductive carboxymethyl cellulose-based hydrogels for flexible wearable strain sensors and arrays. *Carbohydr. Polym.* **2024**, *342*, 122406.
(15) Chen, G.; Zhang, Y.; Li, S.; Zheng, J.; Yang, H.; Ren, J.; Zhu, C.; Zhou, Y.; Chen, Y.; Fu, J. Flexible Artificial Tactility with Excellent Robustness and Temperature Tolerance Based on Organohydrogel Sensor Array for Robot Motion Detection and Object Shape Recognition. *Adv. Mater.* **2024**, *36* (45), No. e2408193.
(16) Wu, X.; Luo, X.; Song, Z.; Bai, Y.; Zhang, B.; Zhang, G., Ultra-Robust and Sensitive Flexible Strain Sensor for Real-Time and Wearable Sign Language Translation. *Adv. Funct. Mater.* **2023**, *33* (36). DOI: 10.1002/adfm.202303504
(17) Li, Y.; Matsumura, G.; Xuan, Y.; Honda, S.; Takei, K., Stretchable Electronic Skin using Laser-Induced Graphene and Liquid Metal with an Action Recognition System Powered by Machine Learning. *Adv. Funct. Mater.* **2024**, *34* (30). DOI: 10.1002/adfm.202313824
(18) Tang, Z.; Meng, L.; Zhang, M.; Shi, Z.; Zhang, K.; Qin, J.; Jiang, L.; Liu, H., An Ultra-Smooth rGO Nano-Thin Film from a Homogeneous Thin Liquid Film Confined by a Conical Fiber Array: Toward the Highly Sensitive Pressure Sensor. *Adv. Funct. Mater.* **2024**, *34* (41). DOI: 10.1002/adfm.202405990
(19) Yuan, T.; Yin, R.; Li, C.; Fan, Z.; Pan, L. Ti3C2Tx MXene-based all-resistive dual-mode sensor with near-zero temperature coefficient of resistance for crosstalk-free pressure and temperature detections. *Chemical Engineering Journal* **2024**, *487*, 150396.
(20) Liu, Y.; Xu, Z.; Ji, X.; Xu, X.; Chen, F.; Pan, X.; Fu, Z.; Chen, Y.; Zhang, Z.; Liu, H.; Cheng, B.; Liang, J. Ag-thiolate interactions to enable an ultrasensitive and stretchable MXene strain sensor with high temporospatial resolution. *Nat. Commun.* **2024**, *15* (1), 5354.
(21) Tang, Z.; Sun, W.; Tao, C.; Peng, T.; Li, H.; Chen, K.; Li, J.; Zhao, Z.; Li, Z.; Hong, X. Rapid response, superior stable, and durable pressure sensor with rGO/CNC interdigital electrode. *Nano Energy* **2024**, *129*, 110041.
(22) Meng, X.; Zhang, C.; Xie, H.; Niu, S.; Han, Z.; Ren, L., A Continuous Pressure Positioning Sensor with Flexible Multilayer Structures Based on a Combinatorial Bionic Strategy. *Adv. Funct. Mater.* **2024**, *34* (17). DOI: 10.1002/adfm.202314479
(23) Stevens, M.; Yun, G.; Hasan, T., Porous Conductive Hybrid Composite with Superior Pressure Sensitivity and Dynamic Range. *Adv. Funct. Mater.* **2024**, *34* (8). DOI: 10.1002/adfm.202309347
(24) Gul, O.; Kim, J.; Kim, K.; Kim, H. J.; Park, I., Liquid-Metal-Based Soft Pressure Sensor and Multidirectional Detection by Machine Learning. *Adv. Mater. Technol.* **2024**, *9* (12). DOI: 10.1002/admt.202302134
(25) Yuan, H.; Zhu, T.; Huang, Y.; Wang, Z.; Han, P.; Tan, L.; Wu, J.; Chen, X.; Yao, P.; Zhu, C.; Xu, J., Hydrophobic and Adhesive Elastomer Encapsulation for Anti-Drying, Non-Swelling, and Adhesive Hydrogels. *Adv. Funct. Mater.* **2024**, *34* (51). DOI: 10.1002/adfm.202409703
(26) Jo, Y.; Lee, Y.; Kwon, J.; Kim, S.; Ryu, G.; Yun, S.; Baek, S.; Ko, H.; Jung, S. 3D active-matrix multimodal sensor arrays for independent detection of pressure and temperature. *Sci. Adv.* **2025**, *11* (3), No. eads4516.
(27) Lee, J. H.; Heo, J. S.; Kim, Y. J.; Eom, J.; Jung, H. J.; Kim, J. W.; Kim, I.; Park, H. H.; Mo, H. S.; Kim, Y. H.; Park, S. K. A Behavior-Learned Cross-Reactive Sensor Matrix for Intelligent Skin Perception. *Adv. Mater.* **2020**, *32* (22), No. e2000969.
(28) Zheng, L.; Hou, X.; Xu, M.; Yang, Y.; Gao, J.; Luo, L.; Zhu, Q.; Li, W.; Wang, X. Scalable Manufacturing of Large-Area Pressure Sensor Array for Sitting Posture Recognition in Real Time. *ACS Mater. Au* **2023**, *3* (6), 669−677.
(29) Shi, L.; Li, Z.; Chen, M.; Qin, Y.; Jiang, Y.; Wu, L. Quantum effect-based flexible and transparent pressure sensors with ultrahigh sensitivity and sensing density. *Nat. Commun.* **2020**, *11* (1), 3529.
(30) Tan, Y.-s.; Han, W.; Wu, Y.; Kuang, D.; Song, L.; Wang, C. Bioinspired, highly sensitive interlocked flexible textile pressure sensor based on multilayer SWCNTs/PVP/rGO dendritic for gesture recognition. *Composites Part B: Engineering* **2024**, *283*, 111639.
(31) Chen, J.; Song, T.; Wang, X.; Zhou, Y.; Wang, T.; Zhang, X.; Zhao, Y.; Yang, B.; Zhang, Y.; Chen, J.; Chen, K.; Li, Y.; Han, W. Ultrasensitive and wide-range MXene/PDMS piezoresistive sensors inspired by rose petals. *Nano Energy* **2024**, *131*, 110285.
(32) Zhao, W.; Li, K.; Li, Z.; Wang, W.; Yu, X.; Zhang, T.; Yang, X., Flexible Pressure Sensor Arrays with High Sensitivity and High Density Based on Spinous Microstructures for Carved Patterns Recognition. *Adv. Funct. Mater.* **2025**, *35* (11). DOI: 10.1002/adfm.202417238
(33) Yang, M.; Cheng, Y.; Yue, Y.; Chen, Y.; Gao, H.; Li, L.; Cai, B.; Liu, W.; Wang, Z.; Guo, H.; Liu, N.; Gao, Y. High-Performance Flexible Pressure Sensor with a Self-Healing Function for Tactile Feedback. *Adv. Sci. (Weinh)* **2022**, *9* (20), No. e2200507.
(34) Zeng, M.; Ding, J.; Tian, Y.; Zhang, Y.; Liu, X.; Chen, Z.; Sun, J.; Wu, C.; Yin, H.; Wei, D.; Fan, H., Phase Separation Manipulated Gradient Conductivity for A High-Precision Flexible Pressure Sensor. *Adv. Funct. Mater.* **2024**, *34* (52). DOI: 10.1002/adfm.202411390
(35) Chen, X.; Luo, Y.; Chen, Y.; Li, S.; Deng, S.; Wang, B.; Zhang, Q.; Li, X.; Li, X.; Wang, C.; He, J.; Tian, H.; Shao, J. Biomimetic Contact Behavior Inspired Tactile Sensing Array with Programmable Microdomes Pattern by Scalable and Consistent Fabrication. *Adv. Sci. (Weinh)* **2024**, *11* (43), No. e2408082.
(36) Li, Y.; Zhang, W.; Zhao, C.; Li, W.; Dong, E.; Xu, M.; Huang, H.; Yang, Y.; Li, L.; Zheng, L.; Mao, M.; Yao, S.; Wang, L.; Ma, J.; Wang, X.; Huang, W. Breaking the Saturation of Sensitivity for Ultrawide Range Flexible Pressure Sensors by Soft-Strain Effect. *Adv. Mater.* **2024**, *36* (36), No. e2405405.
(37) Zhu, H.; Luo, H.; Cai, M.; Song, J. A Multifunctional Flexible Tactile Sensor Based on Resistive Effect for Simultaneous Sensing of Pressure and Temperature. *Adv. Sci. (Weinh)* **2024**, *11* (6), No. e2307693.
(38) Bae, K.; Jeong, J.; Choi, J.; Pyo, S.; Kim, J. Large-Area, Crosstalk-Free, Flexible Tactile Sensor Matrix Pixelated by Mesh Layers. *ACS Appl. Mater. Interfaces* **2021**, *13* (10), 12259−12267.
(39) Li, Y.; Long, J.; Chen, Y.; Huang, Y.; Zhao, N. Crosstalk-Free, High-Resolution Pressure Sensor Arrays Enabled by High-Throughput Laser Manufacturing. *Adv. Mater.* **2022**, *34* (21), No. e2200517.
(40) Yu, J.; Liu, Y.; Niu, Q.; Wang, X.; Yan, X., Visual Piezoresistive Dual-Response Sensor Based on CaZnOS: Mn Mechanoluminescence Materials. *Adv. Mater. Technol.* **2025**, *10* (6). DOI: 10.1002/admt.202401562
(41) Tian, X.; Cheng, G.; Wu, Z.; Wen, X.; Kong, Y.; Long, P.; Zhao, F.; Li, Z.; Zhang, D.; Hu, Y.; Wei, D., High-Resolution Carbon-Based Tactile Sensor Array for Dynamic Pulse Imaging. *Adv. Funct. Mater.* **2024**, *34* (46). DOI: 10.1002/adfm.202406022
(42) Wang, M.; Tu, J.; Huang, Z.; Wang, T.; Liu, Z.; Zhang, F.; Li, W.; He, K.; Pan, L.; Zhang, X.; Feng, X.; Liu, Q.; Liu, M.; Chen, X. Tactile Near-Sensor Analogue Computing for Ultrafast Responsive Artificial Skin. *Adv. Mater.* **2022**, *34* (34), No. e2201962.
(43) Guo, X.; Zhang, T.; Wang, Z.; Zhang, H.; Yan, Z.; Li, X.; Hong, W.; Zhang, A.; Qian, Z.; Zhang, X.; Shu, Y.; Wang, J.; Hua, L.; Hong, Q.; Zhao, Y. Tactile corpuscle-inspired piezoresistive sensors based on (3-aminopropyl) triethoxysilane-enhanced CNPs/carboxylated MWCNTs/cellulosic fiber composites for textile electronics. *J. Colloid Interface Sci.* **2024**, *660*, 203−214.
(44) Zhou, X.; Gu, M.; Li, J.; Li, W.; Zhao, B.; Wang, L.; Wei, L.; Yang, C.; Chen, M. Ultra-broad sensing range, high sensitivity textile pressure sensors with heterogeneous fibre architecture and molecular interconnection strategy. *Chemical Engineering Journal* **2024**, *496*, 154067.
(45) Liu, X.; Ma, Y.; Dai, X.; Li, S.; Li, B.; Zhang, X. Flexible pressure sensor based on Pt/PI network with high sensitivity and high thermal resistance. *Chemical Engineering Journal* **2024**, *494*, 152996.
(46) Choi, S. B.; Noh, T.; Jung, S. B.; Kim, J. W. Stretchable Piezoresistive Pressure Sensor Array with Sophisticated Sensitivity,

Strain-Insensitivity, and Reproducibility. *Adv. Sci. (Weinh)* **2024**, *11* (35), No. e2405374.
(47) Hao, S.; Wang, W.; Ma, C.; Li, X.; Liu, X.; Wang, Y.; Xue, Z.; Xu, F.; Yang, J., A Laminated Strategy Enabled Sustainable Tactile Array with Ultra-Stable Sensory Augmentation. *Adv. Funct. Mater.* **2024**, *34* (51). DOI: 10.1002/adfm.202410360
(48) Gu, M.; Zhao, B.; Gao, J.; Zhou, X.; Huang, L.; Wang, J.; Wei, L.; Yang, C.; Chen, M., Nested-Cell Architecture and Molecular Surface Modification Enabled 10 Megapascals Range High Sensitivity Flexible Pressure Sensors for Application in Extreme Environment. *Adv. Funct. Mater.* **2024**, *34* (33). DOI: 10.1002/adfm.202400494
(49) Xie, H.; Huang, Z.; Wan, J.; Zhou, R.; Chen, T.; Wang, Y.; Cheng, D.; Yang, L.; Ji, J.; Jiang, Y.; Wu, T.; Liu, J.; Pan, T.; Jiang, B.; Zhu, J.; Yao, G.; Gao, M.; Lin, Y., Dual-Band Laser Selective Etching for Stretchable and Strain Interference-Free Pressure Sensor Arrays. *Adv. Funct. Mater.* **2024**, *34* (32). DOI: 10.1002/adfm.202401532
(50) Zhu, W.; Liu, X.; Chen, X.; Chen, K.; Huang, M.; Hu, F.; Zeng, F.; Yu, M.; Chen, M.; Huang, A.; Chen, Z.; Luo, J. Sensitivity−stability trade-off in conductive foam-based pressure sensors. *Journal of Materials Chemistry C* **2024**, *12* (18), 6568−6577.
(51) Yuan, Y.; Xu, H.; Zheng, W.; Liu, M.; Li, S.; Yan, J.; Wang, D.; Liu, K.; Zhang, H.; Chen, G.; Wang, W.; Wu, G.; Xue, C.; Cheng, H.; Gao, L., Bending and Stretching-Insensitive, Crosstalk-Free, Flexible Pressure Sensor Arrays for Human-Machine Interactions. *Adv. Mater. Technol.* **2024**, *9* (5). DOI: 10.1002/admt.202301615
(52) Cao, P.; Wei, J.; Zhang, T.; Deng, H.; Han, Y.; Chen, Z.; Chen, Y.; Guo, Y.; Ma, C., Multifunctional Luffa Sponge Hydrogel with High Mechanical Strength, Fatigue Resistance, and Ionic Conductivity for Monitoring Human Vital Signs. *Adv. Funct. Mater.* **2025**. DOI: 10.1002/adfm.202501131
(53) Liang, J.; Zhang, H.; Zhang, Q.; Liu, Y.; Li, B.; Zang, J.; Cao, X.; Zhang, Z.; Gao, L.; Xue, C. An eco-friendly wood sponge-based multifunctional pressure and temperature sensor for electronic skin. *Journal of Materials Chemistry C* **2024**, *12* (28), 10635−10645.
(54) Wang, Z.; Jiang, S.; Huang, Y.; Song, T.; Liufu, C.; Huang, Y.; Zhou, G.; Zhang, Q.; Qian, X.; Lan, Y.; Attia, N. F., Dual Sensing Signal Decoupling Based on Thermoelectric Polymer Aerogels for Precise Temperature and Pressure Recognition. *Adv. Mater. Technol.* **2024**, *9* (15). DOI: 10.1002/admt.202400096
(55) Ren, J.; Huang, X.; Han, R.; Chen, G.; Li, Q.; Zhou, Z., Avian Bone-Inspired Super Fatigue Resistant MXene-Based Aerogels with Human-Like Tactile Perception for Multilevel Information Encryption Assisted by Machine Learning. *Adv. Funct. Mater.* **2024**, *34* (39). DOI: 10.1002/adfm.202403091

https://doi.org/10.1021/acs.jpclett.5c01566
J. Phys. Chem. Lett. 2025, 16, 9169−9182